



Vieira, L. M. G., Santos, J. C. D., Panzera, T. H., Campos Rubio, J. C., & Scarpa, F. (2017). Novel fibre metal laminate sandwich composite structure with sisal woven core. *Industrial Crops and Products*, 99, 189-195.
<https://doi.org/10.1016/j.indcrop.2017.02.008>

Peer reviewed version

License (if available):
CC BY-NC-ND

Link to published version (if available):
[10.1016/j.indcrop.2017.02.008](https://doi.org/10.1016/j.indcrop.2017.02.008)

[Link to publication record in Explore Bristol Research](#)
PDF-document

This is the accepted author manuscript (AAM). The final published version (version of record) is available online via Elsevier at <https://doi.org/10.1016/j.indcrop.2017.02.008> . Please refer to any applicable terms of use of the publisher.

University of Bristol - Explore Bristol Research

General rights

This document is made available in accordance with publisher policies. Please cite only the published version using the reference above. Full terms of use are available:
<http://www.bristol.ac.uk/pure/about/ebr-terms>

Novel fibre metal laminate sandwich composite structure with sisal woven core

Luciano Machado Gomes Vieira a,b*, Júlio Cesar dos Santos b, Túlio Hallak Panzera b, Juan Carlos Campos Rubio a, Fabrizio Scarpa c

a Department of Production Engineering, Federal University of Minas Gerais, Belo Horizonte, Brazil (*lucianomgv@ufmg.br; juan@ufmg.br)

b Centre for Innovation and Technology in Composite Materials, Department of Mechanical Engineering, Federal University of São João del Rei, Brazil (dsantosjcs@gmail.com; panzera@ufs.edu.br)

c Advanced Composites Centre for Innovation and Science, Department of Aerospace Engineering, University of Bristol, UK. (f.scarpa@bristol.ac.uk)

ABSTRACT

Fibre metal laminates (FMLs) have been widely used to manufacture airframe components. This work describes novel sisal fibre reinforced aluminium laminates (SiRALs) that have been prepared by cold pressing techniques and tested under tensile, flexural and impact loading. The pristine sisal fabric and the sisal fibre reinforced composites (SFRCs) were also tested to understand the difference in mechanical performance of the sisal fibre metal laminates. The SiRALs achieved not only the highest modulus and strength, but also the highest specific properties. The mean specific tensile strength and modulus of the SiRALs reached increases of 132% and 267%, respectively, when compared to the sisal fibre reinforced composites (SFRCs). Moreover, the mean specific flexural strength and modulus of the SiRALs were significantly higher than SFRCs, revealing increases of 430% and 973%, respectively. A delamination fracture mode was noted for SiRALs under bending testing. The SiRALs can be considered promising and sustainable composite materials for structural and multifunctional applications.

Keywords: Fibre Metal Laminates; Sisal fibres; Mechanical properties; Fracture; Composite.

1. Introduction

Fibre Metal Laminates (FMLs) are hybrid composite structures based on thin shells of metal alloys reinforced by fibre polymeric materials (Cortes and Cantwell, 2006). These composites have been used in a wide variety of applications, ranging from the aerospace and the automotive to the biomedical. In comparison to pristine metal sheets, FMLs provide added functionalities such as high specific bending strength, acoustical absorption, vibration transmissibility and damping characteristics (Ochoa and Vaidya, 2011). The low fatigue strength of the aluminium alloys and the problems related to the damage tolerance in fibre reinforced composites has inspired different research groups to develop hybrid structural composite materials able to overcome the limitations of metal and polymeric reinforced composites (Vogelesang and Vlot, 2000). Examples of FMLs developed during the last two decades are the Aramid fibre reinforced Aluminium Laminate (ARALL), the Glass Laminate Aluminium Reinforced Epoxy (GLARE) and the Carbon Reinforced Aluminium Laminates (CARAL) (Sinmazçelik et al., 2011). The first generation of FMLs used in aerospace applications was based on epoxy thermosetting polymer matrices, which offered higher strength and stiffness and enhanced high temperatures performance compared to other polymer matrices. However, thermosetting-based composites are

often brittle and require high processing temperatures and pressures. In comparison, FMLs made from thermoplastic-based composites offer improved toughness and have the potential advantage in manufacturing of requiring short process cycle times. These novel thermoplastic fibre–metal laminates can lead to a rapid and low-cost production of lightweight structural components (Reyes and Kang, 2007).

Increasing environmental concerns have encouraged researchers to develop ranges of recyclable composites based on natural fibres such as jute, kenaf, coir, sisal (Rao et al., 2010; Yusoff, Takagi and Nakagaito, 2016). The application of natural fibres in composite materials has been motivated by the need of producing structures that are environmentally sustainable, cost-effective, recyclable and with biodegradation properties to improve the life cycle of the structural components (Saheb and Jog, 1999; Santos et al., 2015). Natural fibres are also much less abrasive to tooling and moulds compared to synthetic ones. Moreover, sisal fibres exhibit acceptable levels of specific tensile stiffness and strength for structural applications (Silva et al., 2012). The use of natural fibres as reinforcement in structures has rapidly taken place primarily within the automotive industry and in secondary structural designs. Renewable fibres of European origin such as flax and hemp have been used to manufacture door panels and car roofs (Beakou et al., 2008), and truss cores with complex architectures (Cicala et al., 2012). The use of natural fibres in FMLs such as mixed jute/carbon fibres (Vasumathi et al., 2013) and bamboo fibres (Zhang et al., 2000) has been shown to be successful in different applications (Sinmazçelik et al. 2011). A new generation of hybrid sisal fibre composites reinforced with micro and nano particles has been investigated for industrial applications (Silva et al., 2012; Vieira et al., 2016; Ramzy et al., 2014). This work investigates the mechanical properties of FMLs containing an innovative core made of sisal fibre reinforced composite (SFRC). The mechanical results show the potential of SiRALs for industrial applications.

2. Materials and Methods

2.1 Materials

The sisal fabric type plain weave with 1300 g/m² and 2 mm in thickness was supplied by APAEB Sisal (Brazil). The metal part of the SFRC structure consisted in aluminium alloy 2024 T3 with 0.40mm of thickness. The epoxy polymer (Type M) and the hardener (HY951) were supplied by Huntsman (Brazil). Table 1 shows the physical and mechanical properties of the aluminium 2024 T3 (Iaccarino, Langella and Caprino, 2007).

[Table 1]

2.2 Preparation

The sisal fabric (plain weave) in pristine condition was tested without epoxy resin (Fig 1a). The specimen was cut in the weft direction according to the prescribed dimensions recommended by the standard ASTM D3039 (2014). Epoxy polymer was also used at the grip of the sample to avoid slip and possible damage created by the clamps. The SFRCs were manufactured using a hand lay-up technique with a fibre volume fraction of 50%. The composites were compacted at 1500Pa into a metallic mould and cured in an oven at 60°C for 15 hours. Five specimens for each experimental condition plus a replica were prepared (Fig 1c).

[Figure 1]

For the sisal fibre reinforced aluminium laminates (SiRALs), two aluminium alloy plates and the sisal fabric/epoxy core were stacked as shown in Figure 2a, always by

using a hand lay-up process with cold pressing at 1500Pa and subsequent hot curing at 60°C for 15 hours. After curing, the SiRAL was cut in the weft direction using a precision saw to obtain the samples (Figure 2b). The matrix was observed to be distributed homogeneously without an evident presence of internal micro voids (Figure 2c).

[Figure 2]

The SFRCs and SiRALs were subjected to tensile load after 7 days were past of production. The specimen dimensions followed the recommendations of ASTM standard D3039 (2014), with 250mm in length, 25mm in width and 4 mm in thickness. A Shimadzu testing machine (AG-X Plus) with 100kN load cell was used to perform the mechanical tests at 1mm/min, room temperature at 22°C and a humidity level of 60%. The same Shimadzu testing machine was used to carried out the three-point bending tests based on the recommendation of ASTM D7264 (2007). The tests were conducted using a loading speed of 1 mm/min with a same room temperature at 22°C and a humidity level at 60%. The specimen dimensions were set with 300 mm in length, 25 mm in width and 4 mm in thickness.

The SFRCs and the SiRALs were also subjected to impact following the standards ISO 179-1 (2010) and ASTM D6110 (2010). A Charpy impact machine (XJJ series) was used with an energy of 15J and impact speed of 3.8m/s. Samples with 80 mm in length, 12.7 mm in width and 4 mm in thickness were tested at same room temperature (22°C) and humidity (60%). Fractured cross section of the specimens were analysed by the use of an optical microscope.

The fibre metal laminates are defined in base of their metal volume fraction (MVF) which is defined in the following way (Vlot and Gunnink, 2001):

$$MVF = (\sum_{i=1}^n t_{metal}) / t_{laminated} \quad (2)$$

In (2), t_{metal} = thickness of each metal layer, n = number of aluminium layers and $t_{laminated}$ = thickness of total laminate. MVF nearly zero means full composite, while MVF nearly 1 means a monolithic metal (Chai and Manikandan, 2014).

The apparent density of the laminates was calculated as the ratio between the mass of a given volume of the impermeable portion of the material, and the mass of an equal volume of demineralized water at the same temperature (ASTM Standard D792, 2013). A desiccator and a vacuum pump were used to saturate the material with water at 23°C. Five samples for each condition were analysed.

Mesh conversion study was carried out to find a suitable element size, which would achieve a converged solution with reasonable computational time. Non-linear elastic and non- linear plastic uniaxial stresses were modelled using hexahedral elements of type C3D8R with eight nodes.

3. Results and discussion

3.1 Mechanical and Physical properties

The metal volume fractions calculated for SiRALs is 0.18. Table 2 shows the average values of the mechanical and physical properties of the sisal fabric in pristine condition, the sisal fibre reinforced composite (SFRC) and the SiRAL, sisal fibre reinforced aluminium composite.

The addition of aluminium plates (SiRAL) contributed to a percent increase in density of 23.3% compared to SFRCs. As shown in Table 2 the SiRALs achieved

not only the highest modulus and strength, but also the highest specific properties.

[Table 2]

The flexural strengths of the SFRCs and SiRALs were remarkably higher compared to the tensile ones, with increases of 10.7% for the SFRCs, and large augmentations of the strengths compared to the tensile case by 153% for the SiRALs (see Table 2). An immediate explanation about this behaviour is because under tensile loading the entire specimen is subjected to a constant stress, whilst in flexure a relatively small region of the specimen is subjected to the maximum stress (Carrillo, Cantwell, 2009). Besides the difference in the loading volume, the thickness of sandwich composites affects significantly the bending behaviour by the area moment of inertia.

The delamination size increases linearly with time of test, in contrast, the delamination growth rate is constant, independent of the delamination size, and it is only affected by the applied stress (Guo, Wu, Zhang, 1997). When the stresses exceed the ultimate limit, the layers debond and the delaminated area grows, resulting in a reduction of the global stiffness. The process continues up to the point that the panel collapses, which can be readily identified by surface take-off (Remmers and Borst, 2001). The initial delamination can have several causes such as errors in the preparation of the material or inadequate and irregular surface, which are detected and discarded, and in second case a weak interfacial adhesion between the facing and core materials. A weak adhesion between the aluminium plates and the SFRC core was revealed by the presence of delamination failure mode. The physical adhesion between aluminium sheets and epoxy polymer can be significantly enhanced by the use of chemical treatments upon the metallic material, leading to increased roughness (Yiwei et al., 2016).

Previous work has highlighted the importance of materials-based parameters (elastic properties, stacking sequence, volume fraction and bonding condition) and the geometry (pre and post-stretch, size/weight/shape of the pendulum test and speed) in the evaluation of the impact response of FMLs (Vlot and Gunnink, 2001) Table 2 also shows the impact resistance for SFRCs and SiRALs considered in this paper. Three basic types of failure (complete, partial and non-present) are common in sandwich panels under Charpy impact test. A matrix failure is revealed by the presence of a crack in the matrix phase parallel to the fibres; delamination of the laminate layers due to interlaminar stresses; fibre failure such as fibre breakage and fibre buckling; and full penetration of the laminate (Huber et al., 2012).

Figure 3 shows the image of the fractured cross section of SFRC obtained via optical microscope at $\times 4$ magnification. A fragile failure mode was evidenced including rupture of the fibre bundles. In addition, the impact resistance of sisal fibre composites has been observed to be mainly affected by the mechanical properties of the natural fibre reinforcement and its failure mode (Rong et al., 2002).

[Figure 3]

Figure 4 shows the image of the fractured cross section of SiRAL obtained via optical microscope at $\times 4$ magnification presented a hinge failure that is characterized by a partial breakage, with a matrix failure (see yellow arrow), a delamination of the aluminium sheet (blue arrow) and a rupture of the sisal fibre bundle (see green arrow).

[Figure 4]

Figure 5 shows typical stress–strain curves obtained via static tensile testing for the sisal fabric in pristine condition, the SFRC and the SiRAL. The stiffness of the sisal fibres significantly increased after 3% of strain, and the failure occurred at 6%. The failure mode varied considerably, a situation that can be attributed to the physical heterogeneity intrinsic to the natural fibres (Belaadi et al., 2013). A fraying effect was also evident in the fibres aligned along the loading direction (Figure 5b). The tensile strength of the SFRCs varied from 26 MPa to 32 MPa, while the tensile modulus ranged between 2.05 GPa to 2.7 GPa (Table 2). A brittle failure mode was observed for the SFRCs (see Figure 5a), with a maximum strain to failure close to 2.4%. Fibre breakage, along with some fibre pull-out was also identified. Similar results have been observed by Silva, R. et al. (2009), with the brittle failure and fibres instabilities being attributed to poor fibre wettability, the yarns being oriented perpendicularly to the loading direction and also the cross-over positions in the woven fabric, which introduces stress concentration at the yarn's contact surfaces.

[Figure 5]

The tensile strength for the SiRALs varied from 77 MPa to 85 MPa (81.21 ± 4.01), and the correspondent modulus was between 10 GPa and 11 GPa (10.50 ± 0.51). The SiRAL failure is characterized not only by the core failure without delamination (Figure 6a) but also by fibre pull-out with delamination (Figure 6c). The delamination (highlighted by the blue arrows in Figure 6b-d) can be attributed to the weak bonding between the SFRCs and the aluminium plates. A brittle fracture mode in the matrix was also observed (see yellow arrows in Figure 6b-d), as well as fibre pull-out (green arrows in Figure 6b-d). Fraying was observed both along the transverse and parallel direction along the loading. It is worth of notice that for the SFRC the error margin about the average strength was around 14%, while the SiRAL exhibited a much lower error ($\sim 5\%$), indicating that the fibre metal concept provides a stabilisation of the mechanical properties at failure.

[Figure 6]

The SiRAL core was the first to fail, showing a typical lateral gage middle (LGM) failure (ASTM Standard D3039, 2014). A similar behaviour has been also identified by Liu and Xue. (2013) and Liu et al. (2013) when using three different types of thick polyethylene cores.

Figure 7 shows a typical flexural force–displacement curve for the SFRC and the SiRAL. The flexural strength of the SFRCs varied between 28 MPa and 34 MPa (31.39 ± 2.95), and the flexural modulus ranged from 1.7 GPa to 1.9 GPa (1.8 ± 0.12). The average ultimate strain was found at nearly 4.1%. Fibre breakage and pull out were identified to be present at the bottom side of the beams, while a matrix failure was observed at the top beam side.

[Figure 7]

The flexural strength and modulus for the SiRALs varied from 192 MPa to 218 MPa (205.13 ± 12.78), and 22 GPa to 26 GPa (23.8 ± 1.8), respectively. The fracture of the SiRALs composites was characterized by the simultaneous presence of fibre and bottom aluminium plate failures (Figure 7a). In some cases, only part of the sisal core did break with a delamination at the top beam side (Figure 8). No failure was observed at the top aluminium plate in the specimens involved.

[Figure 8]

3.2 General discussions

Compared to the sisal fabric in pristine condition, the tensile stiffness and strength of the SFRCs increased by 230% and 61%, respectively (Table 2). The tensile stiffness and strength of the SiRALS increased by 352% and 186%, respectively, compared to the SFRCs. Further gains in strength and modulus could be achieved by adding chemical treatments in both the sisal fibres and the aluminium plates. Chemical and physical methods have been already used to modify natural fibres and to improve the interface of composite materials (Barreto et al., 2011; D'almeida et al., 2011). The reagent concentration must be adequate to avoid fibre defibrillation, which would negatively affect the mechanical properties of the composite (Sydenstricker, Mochnaz and Amico, 2003)

SiRALS showed a superior tensile modulus and strength compared to the core SFRC. The flexural modulus of SiRALS showed a twelve-time increase in relation to the SFRC specimens (Table 2). The mean flexural strength and modulus achieved for the SiRALS were 205 MPa and 23 GPa, respectively, corresponding to increases of 153% and 1222% over the SFRCs. The impact resistance of the SiRAL composites was 536% higher than the SFRCs. Vlot and Gunnink (2001) have reported that the mechanical properties of the metal alloys are able to affect the energy absorption of FMLs. The aluminium layers in FMLs contribute significantly to yielding of the composite at high load, a stable deformation before the break, high residual strength, the fatigue performance, excellent blunt notch resistance and resistance to short cracks (Chai and Manikandan, 2014).

4. Conclusions

The work described in this paper is related to development and investigation on the mechanical properties of sisal fibre reinforced aluminium laminates (SiRALS) and its core (SFRC). The main conclusions are:

The mean tensile strength and modulus obtained for the SiRALS were 81 MPa and 10.5 GPa, respectively, which correspond to percent increases of 186% and 352% when compared to SFRCs.

The mean flexural strength and modulus achieved for the SiRALS were 205 MPa and 23 GPa, respectively, revealing increases of 153% and 1222% over the SFRCs.

The mean impact resistance of the SiRAL was 142 J/mm², which reveals an increasing of 536% in comparison to the SFRC.

The mean specific tensile strength and modulus of the SiRALS were 132% and 267%, respectively, being both higher than SFRCs.

The mean specific flexural strength and modulus of the SiRALS were higher than SFRCs, revealing percent increases of 430% and 973%, respectively.

A delamination between the aluminium plate and the sisal/epoxy core was often identified during the bending test of SiRALS, showing a weak interfacial adhesion present in these laminates;

This preliminary investigation demonstrates the SiRALS can be considered a promising and sustainable FML for structural engineering applications. Chemical treatments upon the metallic facing material and the sisal fibres will be the scope of future investigations to improve the interfacial adhesion between phases and consequently avoiding delamination and fibre pull-out failure modes, respectively.

Acknowledgements

The authors would like to thank the Brazilian Research Agencies, CNPq, Fapemig and CAPES, for the financial support provided. FS would like to thank the University

of Bristol and ACCIS (Advanced Composites Centre for Innovation and Science) for the logistics support offered during the work.

References

- ASTM Standard D3039 / D3039M, 2014. Standard Test Method for Tensile Properties of Polymer Matrix Composite Materials¹, ASTM International, West Conshohocken, PA.
- ASTM Standard D7264 / D7264M, 2007. Standard Test Method for Flexural Properties of Polymer Matrix Composite Materials, ASTM International, West Conshohocken, PA.
- ASTM Standard D6110 / D6110, 2010. Standard Test Method for Determining the Charpy Impact Resistance of Notched Specimens of Plastics, ASTM International, West Conshohocken, PA.
- ASTM Standard D792 / D792, 2013. Standard Test Methods for Density and Specific Gravity (Relative Density) of Plastics by Displacement, ASTM International, West Conshohocken, PA.
- Barreto, A.C.H., Rosa, D.S., Fachine, P.B. A., Mazzetto, S.E., 2011. Properties of sisal fibres treated by alkali solution and their application into cardanol-based biocomposites. *Compos. Part A Appl. Sci. Manuf.* 2011; 42, 492–500. doi:10.1016/j.compositesa.2011.01.008
- Beakou, A., Ntenga, R., Lepetit, J., Ateba, J.A., Ayina, L.O., 2008. Physico-chemical and microstructural characterization of “*Rhectophyllum camerunense*” plant fibre. *Compos. Part A Appl. Sci. Manuf*; 39, 67–74.
- Belaadi, A., Bezazi, A., Bourchak, M., Scarpa, F., 2013. Tensile static and fatigue behaviour of sisal fibres. *Mater. Des.* 2013; 46, 76–83. doi:10.1016/j.matdes.2012.09.048
- Cicala, G., Recca, G., Oliveri, L., Perikleous, Y., Scarpa, F., Lira, C., Lorato, a., Grube, D.J., Ziegmann, G., 2012. Hexachiral truss-core with twisted hemp yarns: Out-of-plane shear properties. *Compos. Struct.* 2012; 94, 3556–3562. doi:10.1016/j.compstruct.2012.05.020
- Cortes P, Cantwell WJ, 2006. The prediction of tensile failure in titanium-based thermoplastic fibre-metal laminates. *Compos Sci Technol*;66:2306–16. doi:10.1016/j.compscitech.2005.11.031.
- Carrillo, J.G., Cantwell, W.J., 2009. Mechanical properties of a novel fibre–metal laminate based on a polypropylene composite. *Mech. Mater.*;41, 828–838. doi:10.1016/j.mechmat.2009.03.002
- Chai, G.B., Manikandan, P., 2014. Low velocity impact response of fibre-metal laminates - A review. *Compos. Struct.*; 107, 363–381. doi:10.1016/j.compstruct.2013.08.003
- D'almeida A. L. F. S., D'almeida, J. R. M., Barreto, D. W., Calado V., 2011. Effect of surface treatments on the thermal behavior and tensile strength of piassava (*Attalea funifera*) fibres, *Journal of Applied Polymer Science*; 120, 2508–2515. doi:10.1002/app.33349
- Guo, Y.J., Wu, X.R., Zhang, Z.L., 1997. Characterization of delamination growth behaviour of hybrid bonded laminates *Fatigue Fract Eng Mater Struct*, 20 (12), 1699–1708.
- Huber, T., Bickerton, S., Müssig, J., Pang, S., Staiger, M.P., 2012. Solvent infusion processing of all-cellulose composite materials. *Carbohydr. Polym.*; 90, 730–733. doi:10.1016/j.carbpol.2012.05.047

Iaccarino, P., Langella, a, Caprino, G., 2007. A simplified model to predict the tensile and shear stress–strain behaviour of fibreglass/aluminium laminates. *Compos. Sci. Technol.*; 67, 1784–1793. doi:10.1016/j.compscitech.2006.11.005

ISO Standard 179-1:2010 - International Organization for Standardization, *Plastics - Determination of Charpy impact properties.*

Liu, J., Xue, W., 2013. Formability of AA5052/polyethylene/AA5052 sandwich sheets. *Trans. Nonferrous Met. Soc. China*; 23, 964–969. doi:10.1016/S1003-6326(13)62553-4

Liu, J., Liu, W., Xue, W., 2013. Forming limit diagram prediction of AA5052/polyethylene/AA5052 sandwich sheets. *Mater. Des.*; 46, 112–120. doi:10.1016/j.matdes.2012.09.057

Ochoa-Putman C, Vaidya UK., 2011. Mechanisms of interfacial adhesion in metal–polymer composites–Effect of chemical treatment. *Compos Part A Appl Sci Manuf*;42:906–15.Santos, R. P.O., Rodrigues, B. V.M., Ramires, E.C. Ruvolo-Filho, A. C., Frollini, E., 2015. Bio-based materials from the electrospinning of lignocellulosic sisal fibres and recycled PET, *Industrial Crops and Products*, Vol. 72, P. 69-76, ISSN 0926-6690, <http://dx.doi.org/10.1016/j.indcrop.2015.01.024>.

Rong, M.Z., Zhang, M.Q., Liu, Y., Yan, H.M., Yang, G.U.I.C., Zeng, H.M., 2002. Interfacial interaction in Sisal/Epoxy composites and Its Influence on Impact Performance. *Polym. Compos.*; 23, 182–192. doi: 10.1002/pc.10424

Remmers, J.J.C., Borst, R.D., 2001. Delamination buckling of fibre–metal laminates *Compos Sci Technol*, 61, 2207–2213

Reyes, G., Kang, H., 2007. Mechanical behavior of lightweight thermoplastic fibre–metal laminates. *J. Mater. Process. Technol*;186, 284–290. doi:10.1016/j.jmatprotec.2006.12.050

Rao, K.M.M., Rao, K.M., Prasad, A.V.R., 2010. Fabrication and testing of natural fibre composites: Vakka, sisal, bamboo and banana. *Mater. Des.*; 31, 508–513. doi:10.1016/j.matdes.2009.06.023

Ramzy, A., Beermann, D., Steuernagel, L., Meiners, D., Ziegmann, G., 2014. Developing a new generation of sisal composite fibres for use in industrial applications. *Compos. Part B Eng.*; 66, 287–298. doi:10.1016/j.composites.2014.05.016

Saheb, D. N., Jog, J. P., 1999. Natural fibre polymer composites: a review. *Adv Polym Technol*; 18, 351–63. doi: 10.1002/(SICI)1098-2329(199924)18:4<351::AID-ADV6>3.0.CO;2-X

Silva, L.J., Panzera, T.H., Christoforo, A.L., Rubio, J.C.C., Scarpa, F., 2012. Micromechanical analysis of hybrid composites reinforced with unidirectional natural fibres, silica microparticles and maleic anhydride. *Mater. Res.*;15, 1003–1012. doi:10.1590/S1516-14392012005000134

Silva, L.J., Panzera, T.H., Velloso, V.R., Christoforo, A.L., Scarpa, F., 2012. Hybrid polymeric composites reinforced with sisal fibres and silica microparticles. *Compos. Part B Eng.*; 43, 3436–3444. doi:10.1016/j.compositesb.2012.01.026

Silva, R. V., Ueki, M.M., Spinelli, D., Filho, W.W.B., Tarpani, J.R., 2009. Thermal, Mechanical, and hydroscopic behavior of sisal fibre/polyurethane resin-based composites. *J. Reinf. Plast. Compos.*; 29, 1399–1417. doi:10.1177/0731684409102986

Sinmazçelik, T., Avcu, E., Bora, M.Ö., Çoban, O., 2011. A review: Fibre metal laminates, background, bonding types and applied test methods. *Mater. Des.*;32,3671–3685. doi:10.1016/j.matdes.2011.03.011

- Sydenstricker, T.H.D., Mochnaz, S., Amico, S.C., 2003. Pull-out and other evaluations in sisal-reinforced polyester biocomposites. *Polym. Test.*; 22, 375–380. doi:10.1016/S0142-9418(02)00116-2
- Vasumathi, M., Murali, V., 2013. Effect of Alternate Metals for use in Natural Fibre Reinforced Fibre Metal Laminates under Bending, Impact and Axial Loadings. *Procedia Eng.*; 64, 562–570. doi:10.1016/j.proeng.2013.09.131
- Vogelesang LB, Vlot A., 2000. Development of fibre metal laminates for advanced aerospace structures. *J. Mater. Process. Technol.*;103:1–5. doi:10.1016/S0924-0136(00)00411-8
- Vieira, L. M. G., Santos, J. C. d., Panzera, T. H., Christoforo, A. L., Mano, V., Campos Rubio, J. C. and Scarpa, F., 2016. Hybrid composites based on sisal fibres and silica nanoparticles. *Polym Compos.*, doi: 10.1002/pc.23915
- Vlot, A., Gunnink, J. W., 2001. Fibre metal laminates: an introduction. Kluwer Academic Publishers; Dordrecht, Netherlands, doi: 10.1007/978-94-010-0995-9
- Yiwei X., Huaguan L., Yizhou S., Senyun L., Wentao W., Jie T., 2016. Improvement of adhesion performance between aluminum alloy sheet and epoxy based on anodizing technique, *International Journal of Adhesion and Adhesives*, Vol 70, 74-80, ISSN 0143-7496, <http://dx.doi.org/10.1016/j.ijadhadh.2016.05.007>.
- Yusoff, R. B., Takagi, H. Nakagaito, A. N., 2016. Tensile and flexural properties of polylactic acid-based hybrid green composites reinforced by kenaf, bamboo and coir fibres, *Industrial Crops and Products*, Vol 94, P. 562-573, ISSN 0926-6690, <http://dx.doi.org/10.1016/j.indcrop.2016.09.017>.
- Zhang, J.Y., Yu, T.X., Kim, J.K., Sui, G.X., 2000. Static indentation and impact behaviour of reformed bamboo/aluminium laminated composites. *Compos. Struct.*; 50, 207–216. doi:10.1016/S0263-8223(00)00104-5

TABLES

Table 1. Mechanical properties of the aluminium metal sheets 2024 T3.

Designation	Density (g/cm ³)	Elastic modulus (GPa)	Yield stress (MPa)
	Maximum strength (MPa)	Ultimate Strain (%)	
Aluminium 2024 T3	2.70	71.10	381 496 15.90

Table 2. Physical and mechanical properties for sisal fabric, SFRC and SiRAL.

	Sisal Fabric	SFRC	SiRAL
Apparent density (g/cm ³)		0.40±0.020	1.16±0.005 1.43±0.011
Tensile modulus (GPa)		0.70 ±0.05	2.32 ± 0.43 10.50 ±0.51
Specific modulus (GPa/g.cm-3)		1.75	2.00 7.34
Tensile strength (MPa)		17.53±3.05	28.34±4.12 81.21±4.01
Specific strength (MPa/g.cm-3)		43.82	24.43 56.79
Ultimate strain (%)		5.5±0.5	1.8±0.8 3.3±1.1
Flexural modulus (GPa)		-	1.8 ± 0.12 23.8 ± 1.8
Specific modulus (GPa/g.cm-3)		-	1.55 16.64
Flexural strength (MPa)		-	31.39 ± 2.95 205.13 ± 12.78
Specific strength (MPa/g.cm-3)		-	27.06 143.45
Ultimate strain (%)		-	2.81 ± 1.3 2.61 ± 0.4
Impact resistance (J/mm ²)		-	22.40 ± 2.68 142.51 ± 6.72

Figure Captions

Figure 1. Sisal fibre reinforced composites (a) sisal fabric (b) side view, (c) specimens according ASTM D3039 and (d) top view.

Figure 2. SiRAL preparation scheme (Reyes and Kang, 2006).

Figure 3. Fracture of some SFRCs samples: side (a) and top (b) view.

Figure 4. Fracture mode of a SiRAL specimen: (a) side, (b) diagonal and (c) top views.

Figure 5. Tensile stress-strain curve and failure mode of Sisal Fabric, SFRC and SiRAL.

Figure 6. Failure without delamination (a, b) and failure with large delamination (c, d).

Figure 7. Flexural behaviour and failure mode for the (a) SiRAL and (b) SFRC.

Figure 8. Typical fracture of SiRAL after bending test.

Figure 1

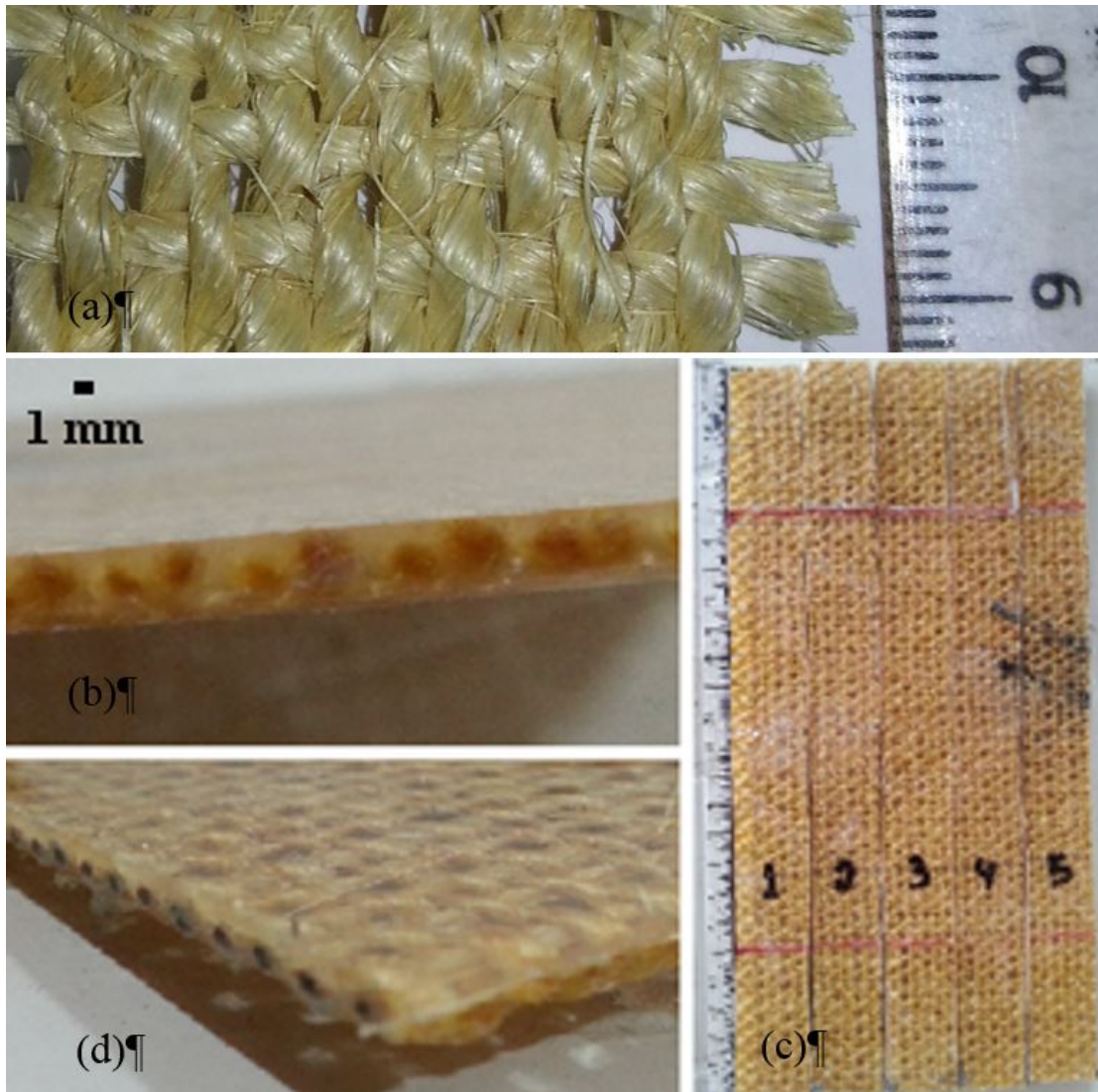


Figure 2

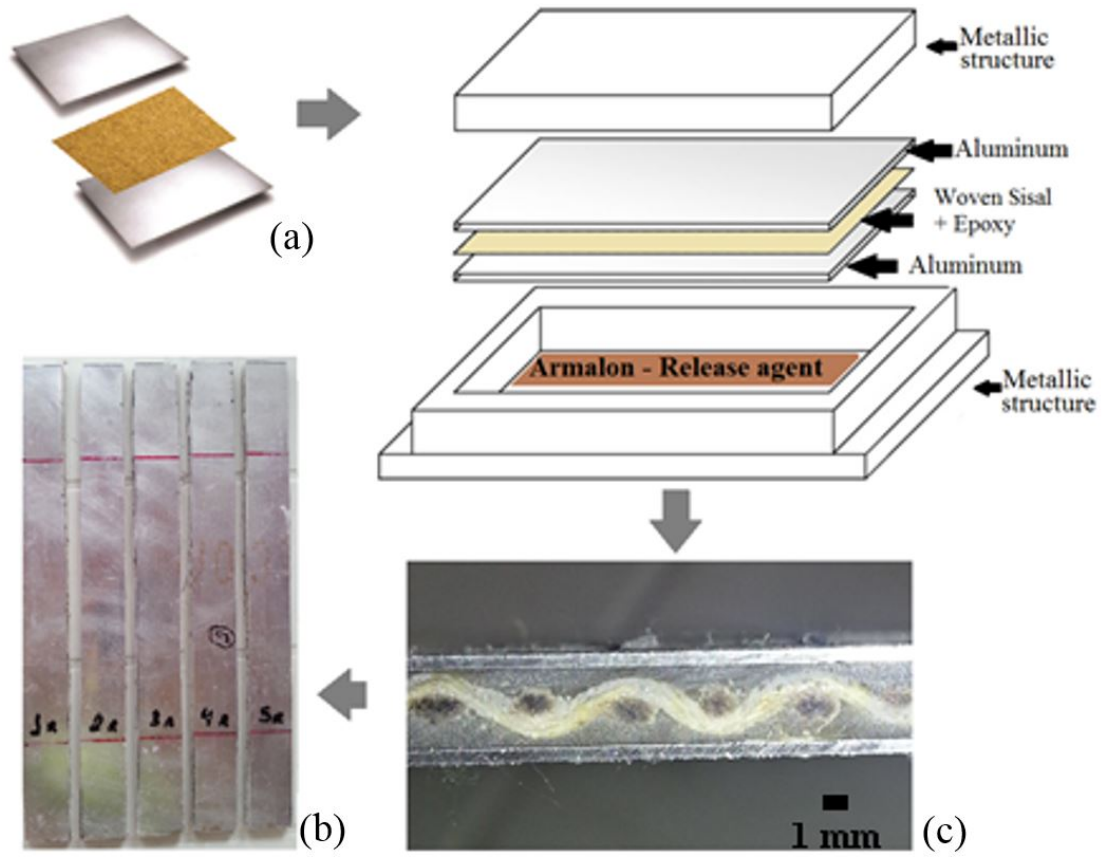
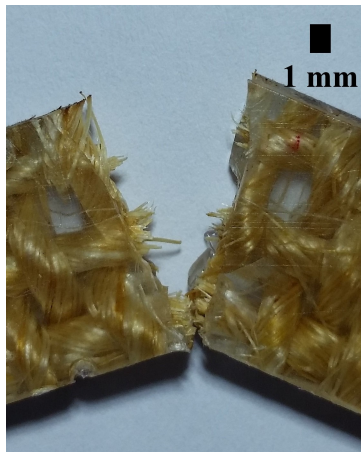


Figure 3



(a)



(b)

Figure 4

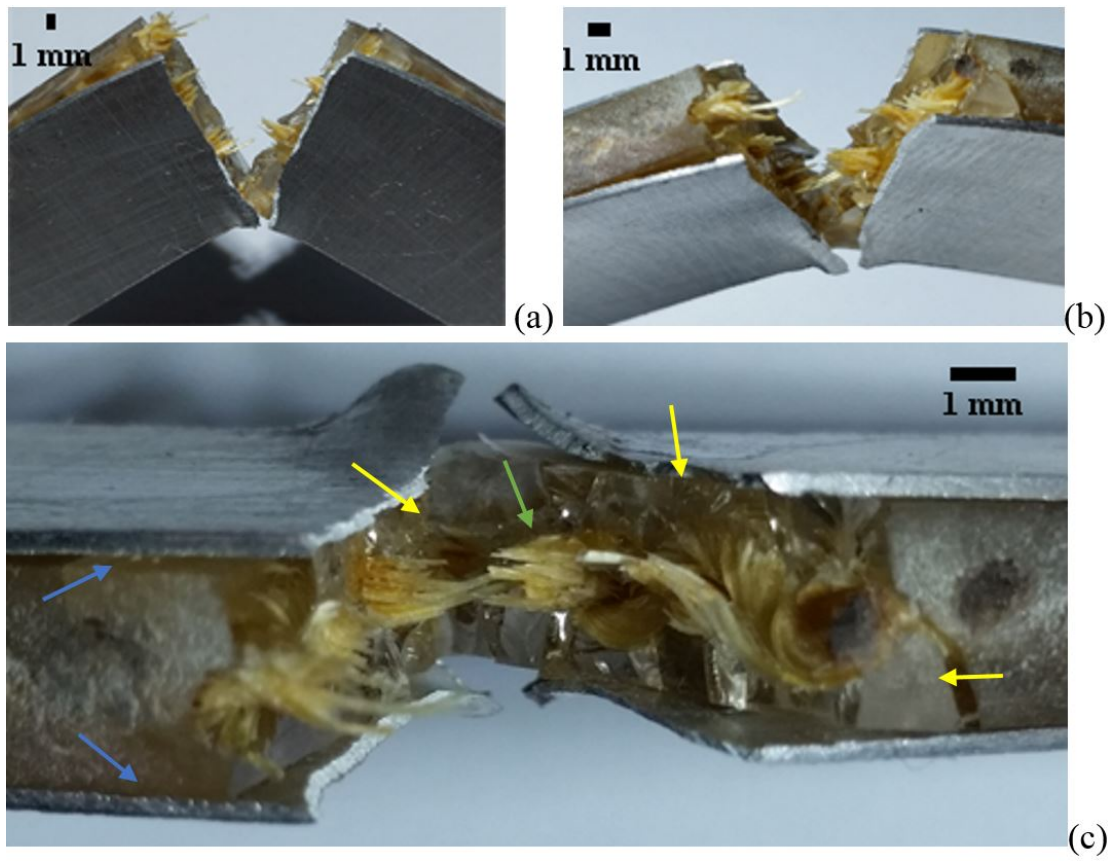


Figure 5

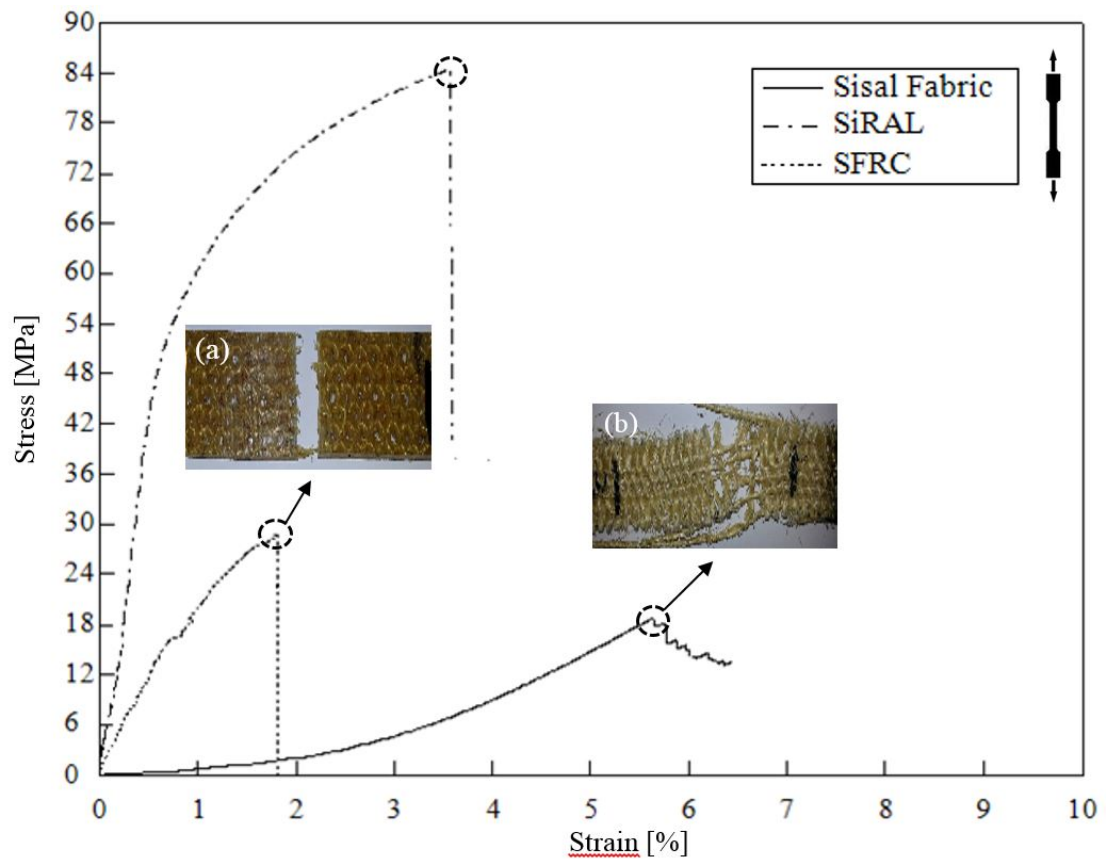


Figure 6

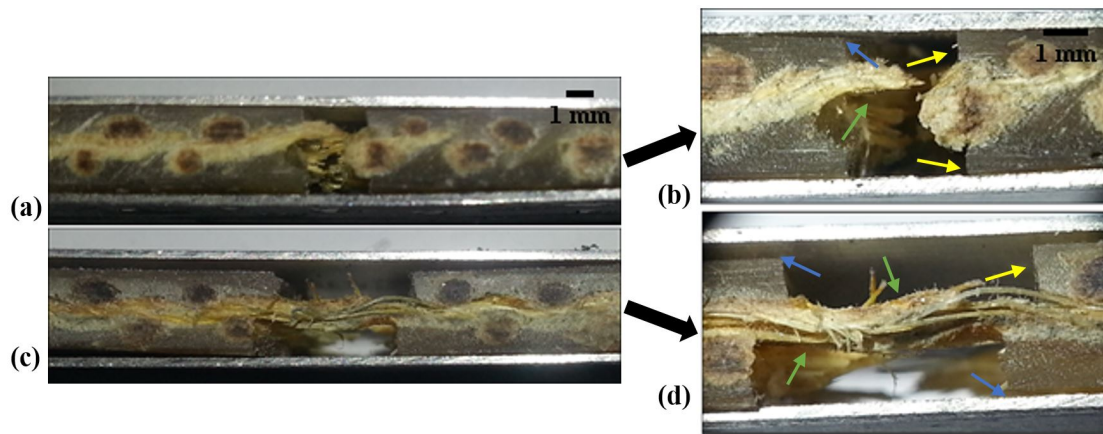


Figure 7

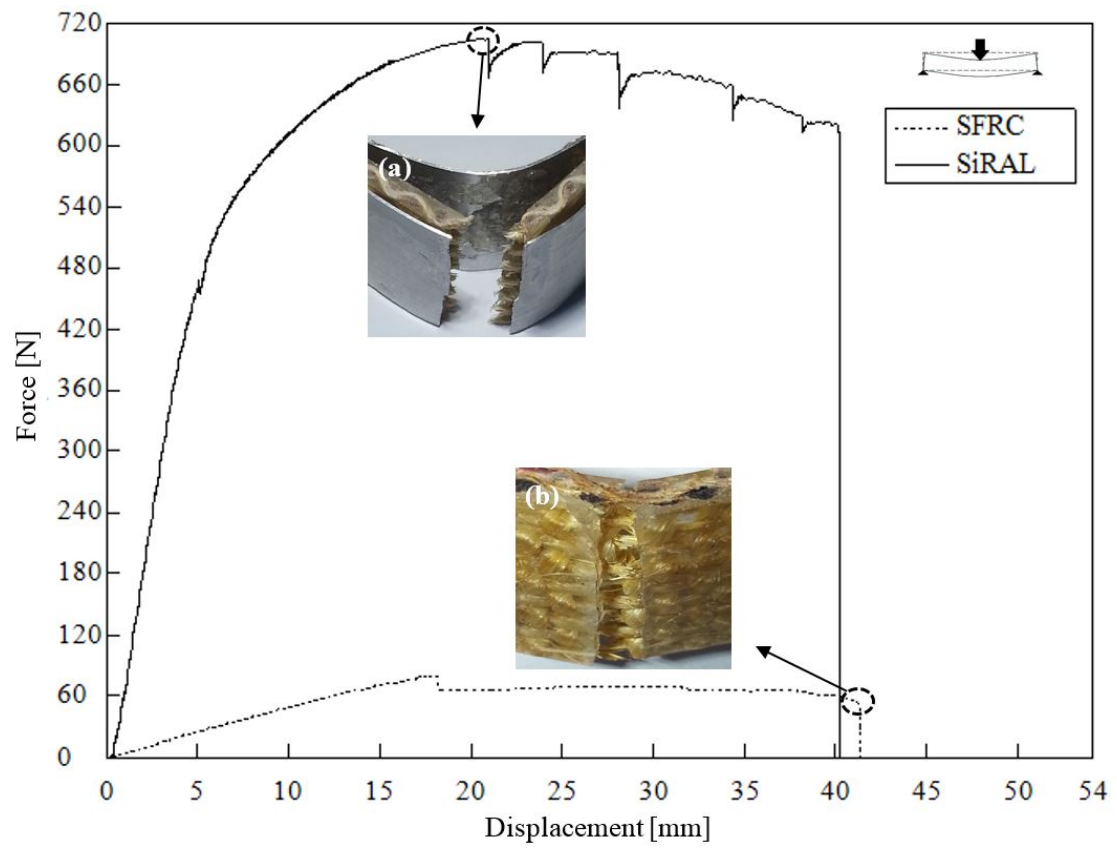


Figure 8

